

Random-phase approximation study of collective excitations in the Bose-Fermi mixed condensate of alkali-metal gases

T. Sogo, T. Miyakawa, T. Suzuki and H. Yabu

Department of Physics, Tokyo Metropolitan University, 1-1 Minamiohsawa, Hachioji, Tokyo

192-0397, Japan

(April 14, 2024)

Abstract

We perform Random Phase Approximation (RPA) study of collective excitations in the Bose-Fermi mixed degenerate gas of Alkali-metal atoms at $T = 0$. The calculation is done by diagonalization in a model space composed of particle-hole type excitations from the ground state, the latter being obtained from the coupled Gross-Pitaevskii and Thomas-Fermi equations. We investigate strength distributions for different combinations of Bose and Fermi multipole (L) operators with $L = 0, 1, 2, 3$. Transition densities and dynamical structure factors are calculated for collective excitations. Comparison with the sum rule prediction for the collective frequency is given. Time dependent behavior of the system after an external impulse is studied.

I. INTRODUCTION

Collective excitation is one of the most prominent phenomena in quantum many-body systems such as liquid helium, electron gas, nucleus, etc. In the recently developed Bose-Einstein condensates of trapped atomic gases [1,2], collective oscillations were the first of the dynamical phenomena discovered [3]. Collective oscillations are characterized by various quantum numbers related to, e.g., the shape of oscillation, or internal degrees of freedom of the constituents such as spin, isospin, etc. The oscillation frequency, the damping width, etc. depend on the interparticle interaction of the constituents, and thus provide a clue to unravel the dynamical correlation of the many-body system.

Study of the properties of trapped neutral atoms has been extended to fermi systems [4] where the occurrence of the Fermi degeneracy was observed, and also to the mixture of bosons and fermi particles. The latter system with condensed bosons and degenerate fermions was recently realized experimentally [5,6]. This system is one of the typical example in which particles obeying different statistics are intermingled. Theoretical studies of the boson-fermi mixed system of cold atomic gases have been done for static properties [7-12], for the phase diagram and phase separation [13-15], for the stability of the system [16,17] and for collective excitations [18-20].

In Ref. [18] sum rule approach has been applied for collective excitations in the boson-fermi mixed system. Average excitation energies for the states with multipoles $L = 0; 1; 2$ were calculated for both in-phase and out-of-phase modes of the bosons and the fermi particles, and the dependence on the boson-fermi interaction strength was studied. The sum rule approach is a powerful technique for collective states in quantum many-body systems, and has been successfully applied to the excitation of boson condensed systems, see Refs. [2,21]. It does not give, however, direct information on the eigenstates of the system, but rather an average behavior of the strength distribution for the adopted multipole excitation operator. For a more detailed investigation on the dynamical properties of the system, one would need a study of individual eigenstates.

In the present paper we extend the previous study [18] of collective excitations in the bose-fermion mixed system. We calculate full particle-hole type excitations by diagonalization of an RPA type matrix. The motive of this calculation is threefold: first of all, the calculation allows us to study the excitation spectrum and the strength distribution in contrast to the sum rule method which focuses on the strength weighted average of the prescribed multipole operators. We study, for instance, the degree of collectivity of the excitations depending on the strength of boson-fermion interaction, and estimate the damping of the collective excitation albeit within the space of particle-hole excitations. Information on the wave function allows us to calculate observables such as the dynamical structure factor. The latter for bose-condensed systems is now becoming available experimentally by two-photon spectroscopy [22] and is being studied theoretically [23]. Secondly, we compare the results with those obtained from the sum rule approach. This provides a check on the approximation adopted in the calculation such as the model space truncation. The comparison also allows one to examine the structure of the low- and high-lying collective modes which was speculated in [18] through the mixing angle of multipole operators. Third, we can predict the time-dependent behavior of the system for a given external perturbation. This process is actually the one that has been employed in the previous experimental study of collective excitations in BEC. An RPA study of the bose-fermion mixed system has recently been done in [20], where the response for an external multipole field is formulated in the form of an integral equation. In the present calculation we approach the problem by diagonalizing the RPA matrix, by incorporating the discrete nature of the excitation in an isolated trapped system, and investigate, in particular, the properties of the strength distribution for a combination of bose and fermion operators and for various values of the bose-fermion interaction strengths.

The content of the paper is as follows: in the next section we derive the RPA equation for the bose-fermion mixed system using the equation of motion for particle-hole type excitation operators. The single particle (hole) states are obtained in the mean-field calculation, i.e., by solving the coupled Gross-Pitaevskii and Thomas-Fermi equations. In Section III we

rst briefly describe the parameters and the numerical procedure employed in the present calculation. We then turn to the detailed studies of the results obtained, including ground state density, single particle states, and strength distribution for each multipole. Comparison with the sum rule calculation is given. Transition densities and dynamical structure factors for some of the collective excitations are presented. We finally consider the time development of the system after an external multipole impulse on the system. Last section is devoted to summary and conclusion.

II. FORMULATION

We consider a dilute spin-polarized boson-fermion mixed system trapped in a spherically symmetric harmonic oscillator potential at $T = 0$. The system is described by the Hamiltonian

$$\hat{H} = \hat{H}_0 + \hat{V}_b + \hat{V}_{bf} \quad (1)$$

with

$$\begin{aligned} \hat{H}_0 &= \int d^3r \left[\frac{\hbar^2}{2m} \nabla^2 \hat{\psi}^\dagger \hat{\psi} + \frac{1}{2} m \omega_0^2 r^2 \hat{\psi}^\dagger \hat{\psi} \right] + \int d^3r \left[\frac{\hbar^2}{2m} \nabla^2 \hat{\chi}^\dagger \hat{\chi} + \frac{1}{2} m \omega_0^2 r^2 \hat{\chi}^\dagger \hat{\chi} \right]; \\ \hat{V}_b &= \frac{1}{2} g_{ZZ} \int d^3r d^3r' \hat{\psi}^\dagger(\mathbf{r}) \hat{\psi}(\mathbf{r}') \hat{\chi}^\dagger(\mathbf{r}) \hat{\chi}(\mathbf{r}'); \\ \hat{V}_{bf} &= h \int d^3r d^3r' \hat{\psi}^\dagger(\mathbf{r}) \hat{\psi}(\mathbf{r}') \hat{\chi}^\dagger(\mathbf{r}) \hat{\chi}(\mathbf{r}'), \end{aligned} \quad (2)$$

where $\hat{\psi}$ and $\hat{\chi}$ are the boson and the fermion field operators. We take, for simplicity, the mass m and the trapping frequency ω_0 to be the same for the boson and the fermion. The boson-boson and the boson-fermion interaction strengths for the pseudopotentials, g and h , are related to the s-wave scattering lengths a_{bb} and a_{bf} through $g = 4\pi\hbar^2 a_{bb}/m$, $h = 4\pi\hbar^2 a_{bf}/m$, while the fermion-fermion interaction is omitted as we consider a polarized dilute system at low temperature.

According to the Landau picture of quantum liquid, low lying excited states of the system may be described by quasiparticle excitations which have the structure of particle-hole (p-h) type excitations from the ground state. Small amplitude collective oscillations of the

system, corresponding to the zero sound, are given by the coherent superposition of these p-h excitations and are well described by RPA for any fermion systems. The corresponding excitations in the Bose condensed system have been formulated in the Bogoliubov-de Gennes type equation. The latter is essentially the same as the one obtained in RPA, and we consider below the two types of excitations on the same footing.

In order to formulate RPA for the Bose-fermion mixed system, we first determine the ground state in the mean field approximation. The obtained mean field provides us with single particle energies and wave functions. Let us expand the field operators in terms of a complete set of single particle wave functions as

$$\hat{\psi}(\mathbf{r}) = \sum_k \psi_k(\mathbf{r}) b_k; \quad \hat{\psi}(\mathbf{r}) = \sum_k \psi_k(\mathbf{r}) a; \quad (3)$$

where b_k and a are the boson and the fermion annihilation operators in the single particle states specified by the wave functions ψ_k and ψ . They satisfy the standard commutation or anticommutation relations. The single particle states with quantum numbers k or f are determined by minimizing the energy expectation value. The trial wave function of the system is given by the product of N_b bosons in a single state $\psi_{k=0}(\mathbf{r})$ and the Slater determinant of N_f different fermionic states $\psi_f(\mathbf{r})$. From the stationary condition of energy for the variation of these wave functions with a given number of bosons N_b and fermions N_f , we obtain the set of coupled equations, i.e., the Gross-Pitaevskii equation for the boson wave function

$$\left[-\frac{\hbar^2}{2m} \nabla^2 + \frac{1}{2} m \omega_0^2 r^2 + g N_b \psi_{k=0}(\mathbf{r}) \psi_{k=0}^*(\mathbf{r}) + \hbar \sum_f \psi_f(\mathbf{r}) \psi_f^*(\mathbf{r}) \right] \psi_{k=0}(\mathbf{r}) = E_{k=0} \psi_{k=0}(\mathbf{r}) \quad (4)$$

and the mean-field equation for the occupied fermion states

$$\left[-\frac{\hbar^2}{2m} \nabla^2 + \frac{1}{2} m \omega_0^2 r^2 + \hbar N_b \psi_{k=0}(\mathbf{r}) \psi_{k=0}^*(\mathbf{r}) \right] \psi_f(\mathbf{r}) = E_f \psi_f(\mathbf{r}); \quad (5)$$

where

$$\psi_f(\mathbf{r}) = \sum_{j \text{ occupied}} \psi_j(\mathbf{r}) f_j \quad (6)$$

is the ground state density of fermions, μ_b is the boson chemical potential and ϵ_f are the single particle energies for the fermion. Set of equations (4) and (5) together with the fermion number condition

$$\int d^3r \rho_f(\mathbf{r}) = N_f \quad (7)$$

constitute a closed set of equations. The single particle wave functions are normalized to unity. In Eq. (4) we approximate the factor $N_b - 1$ by N_b . Once the single particle wave functions for the occupied states are obtained from Eqs. (4) and (5), the wave functions of the unoccupied states are calculated from a similar set of equations, i.e.,

$$-\frac{\hbar^2}{2m} \nabla^2 \psi_k + \frac{1}{2} m \omega_0^2 r^2 + g N_b \psi_0(\mathbf{r}) \psi_k + \epsilon_f(\mathbf{r}) \psi_k = \epsilon_{k,b}(\mathbf{r}) \psi_k \quad (8)$$

for bosons with $k \neq 0$, and the same equation (5) for fermions but for unoccupied states. Orthogonality of these wave functions to the occupied ones are automatically satisfied [24].

For a large number of particles with a smooth mean field potential, the Thomas-Fermi calculation provides a good approximation. Assuming this to be the case, we determine the fermionic ground state density ρ_f by using

$$\frac{\hbar^2}{2m} (\nabla^2 \rho_f)^{2/3} + \frac{1}{2} m \omega_0^2 r^2 + \hbar N_b \psi_0(\mathbf{r}) \psi_f = \epsilon_F \quad (9)$$

together with the equation (4) instead of fully solving the coupled set of equations (4) and (5). The Fermi energy ϵ_F is determined by integrating the density $\rho_f(\mathbf{r})$ so as to give the fermion number. Numerical consistency of this procedure will be shown in the next section. With ρ_f and ψ_0 so determined, the wave functions ψ_k ($k \neq 0$) and ψ_f are obtained as described above.

We assume below that the mean field is spherically symmetric, and the single-particle quantum numbers n and k involve standard radial and angular momentum quantum numbers $(n; l; m)$. (Note that the spin quantum number is frozen.) We consider the case in which the fermionic ground state (Slater determinant) is m -closed and thus is consistent with the spherically symmetric mean field. We denote by $p(n)$ the fermion single particle states

unoccupied (occupied) in the Slater determinant, i.e., those above (below) the Fermi energy ϵ_F . For the bosons at $T = 0$ the occupied state is the lowest single-particle state $k = 0$.

We now define the creation and annihilation multipole operators of the excited state $|jLM\rangle$ with angular momentum quantum numbers L, M and an additional quantum number j :

$$Q_{LM}^Y = F_{LM}^Y + B_{LM}^Y; \quad (10)$$

$$F_{LM}^Y = \sum_{ph} \sum_{m_p m_h} X_{phL}^Y h_{p h}^{LM} \langle jLM | i \rangle (-1)^{m_h} a_{p m_p}^Y a_{h m_h}^Y + \sum_{ph} \sum_{m_p m_h} Y_{phL}^Y h_{h p}^{LM} \langle jLM | i \rangle (-1)^{m_p} a_{h m_h}^Y a_{p m_p}^Y; \quad (11)$$

$$B_{LM}^Y = \frac{1}{N_b} \sum_{k \neq 0} \sum_{m_k} U_{kL}^Y b_{k m_k}^Y + \sum_{kL} V_{kL}^Y (-1)^{L+M} b_{0 kL-M}^Y; \quad (12)$$

where X, Y, U, V are the amplitudes to be determined in RPA, and $h_{p h}^{LM} \langle jLM | i \rangle$ is the Clebsch-Gordan coefficient.

In RPA the operator Q is determined so as to satisfy the equation of motion

$$[H, Q_{LM}^Y] = \hbar Q_{LM}^Y; \quad (13)$$

where the terms in the l.h.s. which involve different combination of operators $a^Y; a; b^Y; b$ from that in Q^Y are neglected by the assumption of RPA. The state

$$|jLM\rangle = Q_{LM}^Y |i\rangle \quad \text{with} \quad Q_{LM}^Y |i\rangle = 0 \quad (14)$$

is then an approximate eigenstate of the Hamiltonian together with the correlated ground state given by $|i\rangle$. The amplitudes satisfy the orthonormality condition

$$\sum_{ph} (X_{phL}^Y X_{phL}^0 + Y_{phL}^Y Y_{phL}^0) + \sum_{k \neq 0} (U_{kL}^Y U_{kL}^0 + V_{kL}^Y V_{kL}^0) = 0; \quad (15)$$

Substituting Eq. (10) into Eq. (13) we obtain the eigenvalue equation in matrix form:

$$\begin{pmatrix} 0 & 1 & 0 & 1 \\ A_{XX} & A_{XU} & B_{XY} & B_{XV} \\ A_{UX} & A_{UU} & B_{UY} & B_{UV} \\ B_{XY} & B_{XV} & A_{XX} & A_{XU} \\ B_{UY} & B_{UV} & A_{UX} & A_{UU} \end{pmatrix} \begin{pmatrix} X \\ U \\ Y \\ V \end{pmatrix} = \hbar \begin{pmatrix} X \\ U \\ Y \\ V \end{pmatrix}; \quad (16)$$

where submatrices A and B are given by

$$\begin{aligned}
(A_{XX})_{ph,p'h^0} &= \begin{bmatrix} f_{p_b} & f_{h_{b^0}} \end{bmatrix} p_{p^0} h_{p^0} p_{h^0} h_{h^0}; \\
(A_{XU})_{ph;k} &= \frac{h}{4} \frac{p}{N_b} \frac{\hat{l}_p \hat{l}_h}{\hat{L}} (1)^{h_{p^0} h_{h^0} l_{p^0} l_{h^0} l_0} drr^2 R_{p_b}^f R_{h_{b^0}}^f R_{k_L}^b R_{00}^b; \\
(A_{UX})_{k,ph} &= (A_{XU})_{ph;k}; \\
(A_{UU})_{k,k^0} &= \begin{bmatrix} b_{k_L} & b_{k^0} \end{bmatrix} k k^0 + \frac{g N_b}{4} \frac{Z}{drr^2} R_{k_L}^b R_{k^0_L}^b R_{00}^b R_{00}^b; \\
(B_{XY})_{ph,p'h^0} &= 0; \\
(B_{XV})_{ph;k} &= \frac{h}{4} \frac{p}{N_b} \frac{\hat{l}_p \hat{l}_h}{\hat{L}} (1)^{h_{p^0} h_{h^0} l_{p^0} l_{h^0} l_0} drr^2 R_{p_b}^f R_{h_{b^0}}^f R_{k_L}^b R_{00}^b; \\
(B_{UY})_{k,ph} &= (B_{XV})_{ph;k}; \\
(B_{UV})_{k,k^0} &= \frac{g N_b}{4} (1)^{l_{k^0}} \frac{Z}{drr^2} R_{k_L}^b R_{k^0_L}^b R_{00}^b R_{00}^b
\end{aligned} \tag{17}$$

with $\hat{l} = \frac{p}{2l+1}$. In Eq. (17) $R_{n1}^b(r)$ and $R_{n1}^f(r)$ are the radial parts of the single particle wave functions and , which are defined by $_{n1m}(\mathbf{r}) = R_{n1}^b(r) Y_m(\theta; \phi)$ and $_{n1m}(\mathbf{r}) = R_{n1}^f(r) Y_m(\theta; \phi)$ where $Y_m(\theta; \phi)$ are the spherical harmonics. We omitted $O(N_b^{-1})$ terms in this calculation. Actually we obtain the same set of equations if we replace $b_0^y; b_0$ in Eq. (12) with $\frac{p}{N_b}$, which is equivalent to the Bogoliubov-de Gennes equation for the bosonic system.

The response of the system to an external field is represented by the transition matrix elements of the relevant operators which connect the ground state and an excited state. The external probe for a collective oscillation is assumed to be long-ranged and is given by the standard multipole operators, i.e.,

$$F_L(\mathbf{r}) = \begin{cases} \frac{1}{4} r^2 & (L=0) \\ r^L Y_{L0}(\theta) & (L \neq 0) \end{cases} \tag{18}$$

As the system is composed of two kinds of particles, we define operators

$$F_L^b = \int d^3r \hat{\gamma}(\mathbf{r}) F_L(\mathbf{r}) \hat{\gamma}(\mathbf{r}); \quad F_L^f = \int d^3r \hat{\gamma}(\mathbf{r}) F_L(\mathbf{r}) \hat{\gamma}(\mathbf{r}) \tag{19}$$

and their combination

$$F_L = F_L^f - F_L^b; \tag{20}$$

where F_L with $= f; b; +; -$ are respectively called 'fermionic', 'bosonic', 'in-phase' and 'out-of-phase' type operators. The transition amplitudes for these operators are calculated in RPA as:

$$\langle 0 | F_L | L \rangle = \langle 0 | F_L^f; Q_{L0}^Y | 0 \rangle = \langle 0 | F_L^f; F_{L0}^Y | 0 \rangle - \langle 0 | F_L^b; B_{L0}^Y | 0 \rangle; \quad (21)$$

$$\langle 0 | F_L^f; F_{L0}^Y | 0 \rangle = \sum_{ph} \frac{1}{4} \frac{\hat{p}_h}{\hat{L}} \langle 0 | 0 \rangle \langle 0 | 0 \rangle \left[(-1)^h X_{phL} + (-1)^b Y_{phL} \right] \int dr r^2 R_{hL}^f(r) R_{pL}^f(r); \quad (22)$$

$$\langle 0 | F_L^b; B_{L0}^Y | 0 \rangle = \sum_k \frac{1}{4} \frac{\hat{N}_b}{\hat{L}} \left[U_{phL} + (-1)^b V_{phL} \right] \int dr r^2 R_{kL}^b(r) R_{00}^b(r); \quad (23)$$

where $= 2$ for $L = 0$ and $= L$ for $L \neq 0$. The strength distribution for the multipole operator F_L is then given by

$$S_L = \sum_{(f; b; +; -)} |\langle 0 | F_L | L \rangle|^2; \quad (= f; b; +; -) \quad (24)$$

They measure the collectivity of the excited states with respect to the multipole operator which characterizes the shape (or volume for $L = 0$) oscillation of the system.

More detailed information on the structure of the collective excitation may well be represented by the transition densities [25]

$$\langle 0 | \hat{\rho}(\mathbf{r}) | LM \rangle = \sum_L Y_{LM}(\theta, \phi) \rho_L(r); \quad (= f; b); \quad (25)$$

$$\rho_L^f(r) = \sum_{ph} \frac{1}{4} \frac{\hat{p}_h}{\hat{L}} \langle 0 | 0 \rangle \langle 0 | 0 \rangle \left[(-1)^h X_{phL} + (-1)^b Y_{phL} \right] R_{hL}^f(r) R_{pL}^f(r); \quad (26)$$

$$\rho_L^b(r) = \sum_k \frac{1}{4} \frac{\hat{N}_b}{\hat{L}} \left[U_{phL} + (-1)^b V_{phL} \right] R_{kL}^b(r) R_{00}^b(r); \quad (27)$$

where $\hat{\rho}^f(\mathbf{r}), \hat{\rho}^b(\mathbf{r})$ are the fermion and boson density operators:

$$\hat{\rho}^f(\mathbf{r}) = \hat{\psi}^\dagger(\mathbf{r}) \hat{\psi}(\mathbf{r}); \quad \hat{\rho}^b(\mathbf{r}) = \hat{\psi}^\dagger(\mathbf{r}) \hat{\psi}(\mathbf{r}); \quad (28)$$

Recent development of the two-photon Bragg spectroscopy [22] allows us to obtain dynamical structure factors (response function) for the excitations in trapped atomic gases. They are related to the transition densities as

$$S_L(q) = \sum_L |F_L(q)|^2; \quad (29)$$

$$F_L(q) = \int dr r^2 \rho_L(qr) \rho_L(r); \quad (30)$$

where q denotes momentum transferred to the system and $j_L(qr=h)$ are spherical Bessel functions of order L . The long wavelength limit of the dynamical structure factor is proportional to the strength distribution for the multipole operators defined above.

III. CALCULATION

A. Numerical procedure

We consider a boson-fermion mixture of potassium isotopes, i.e., ^{41}K (boson) and ^{40}K (fermion). We take the same value $m = 0.649 \times 10^{-25} \text{ kg}$ for the boson and the fermion masses. The boson-boson interaction strength g is obtained from the scattering length $a_{bb} = 15.13 \text{ nm}$ for ^{41}K - ^{41}K [26], while the boson-fermion interaction strength h is varied. (A negative value for the scattering length a_{bf} for ^{40}K - ^{41}K has been suggested in [26], although not well established yet.) Both particles are assumed to be trapped in the spherical oscillator potential with the same trap frequency $\omega_0 = 100 \text{ Hz}$. The oscillator length $\ell_0 = \sqrt{\frac{\hbar}{m\omega_0}}$ is 4.03 nm for the adopted value of ω_0 .

Number of bosons is fixed at $N_b = 1000$, while that of fermions is calculated in the Thomas-Fermi approximation for a fixed Fermi energy $\epsilon_F = (6 \times 1140)^{1/3} \hbar \omega_0$. The latter is determined so that the last oscillator shell with a number of quanta $N = 2n + \ell$ is given by $N_{\text{Fermi}} = 17$ at $h=g=0$. This gives the number of fermions $N_f = 1140$ at $h=g=0$. N_f is dependent on the boson-fermion interaction strength, and it is assumed that all the subshells given by the quantum numbers $(n; \ell)$ are m -closed, which gives, for instance, $N_f = 1050$ at $h=g=8$ and $N_f = 1227$ at $h=g=6$ for the given value of ϵ_F .

The single-particle wave functions were obtained from the coupled Gross-Pitaevskii and Thomas-Fermi equations by expanding the wave functions in the harmonic oscillator basis for the given oscillator constant. We included associated Laguerre functions L_n up to $n = 30$ for fermions and $n = 15$ for bosons.

The excitation energies and the wave functions for each multipole L are obtained by

diagonalization of the RPA matrix. To construct the particle-hole basis we included single particle states for bosons up to $n = 7$ for $\lambda = 0$ and $n = 6$ for $\lambda = 1; 2; 3$, so that seven p-h configurations are included for each $L = 0; 1; 2; 3$. For fermions, four (particle) states above the Fermi level ϵ_F and up to four (hole) states below ϵ_F have been included for each λ . The number of fermi-p-h configurations is 240 for monopole, 464 for dipole, 672 for quadrupole and 1124 for octupole. The dimension of the RPA matrix is twice the sum of boson and fermi configurations for each multipole. The number of boson configurations is the same for the four multipoles considered in the present calculation.

B . Static properties

In the ground state the fermion density distribution is much broader than that for the boson due to Fermi pressure [9,17], although at large negative value of $h=g$ the boson-fermion attraction tends to produce a larger overlap of the two kinds of particles as shown in Ref. [17]. As the boson-fermion interaction becomes repulsive the fermions are squeezed out from the central part. This in turn causes a smaller overlap of bosons and fermions, and thus a relatively small net effect of the interaction on the binding energy. For the present choice of parameters the fermions are distributed outside of the boson 'core' around $h=g = -7$, forming a 'shell' like structure [7,8,13,17]. Note that this behavior would be changed if one adopts different values for $N_f=N_b$ and g , which may be represented by a single parameter introduced in Ref. [9].

The condition for the validity of the Thomas-Fermi approximation used to obtain the above fermion density distribution may be expressed in terms of the local de Broglie wavelength $\lambda(r) = h/p(r)$, where $p(r) = \sqrt{2m(\epsilon_F - V_e(r))}$ with fermion mean field potential $V_e(r) = \frac{1}{2}m\omega_0^2 r^2 + h_b(r)$. With this quantity, the condition becomes [27]

$$f(r) = \frac{d\lambda(r)}{dr} \ll 1: \quad (31)$$

At $h=g = -8$ where the fermionic potential may have a most pronounced structure, the value of $f(r)$ is $\sim 10^{-2}$ except around turning points. At the turning points, however, the fermion

density produces only a negligible influence on the mean field potential. The validity of the present Thomas-Fermi calculation may also be checked by comparing the fermion density distribution $\rho_f(r)$ obtained from Eq. (9) with the one calculation from the single particle wave functions according to Eq. (5). The comparison of the two distribution in the range $h=g = 6 \text{--} 8$ shows that they agree within the order of 10^2 over the entire radial range, suggesting the consistency of the present calculation.

In Fig. 1 we show the fermion single-particle energies measured from Fermi energy, ϵ_F , against orbital angular momentum l for three values of the interaction parameter, $h=g = 5.0; 1.0; -3.0$. The Fermi energy ϵ_F is denoted by the horizontal line at zero energy. Note that ϵ_n are given by those of the harmonic oscillator at $h=g = 0$, $\epsilon_n = (2n + \frac{1}{2})\hbar\omega$, as we have no direct interaction among fermions. One should note also that the yrast state, i.e., the lowest state for each angular momentum l , has no radial node, and the yrare one, the second lowest state, has one radial node, etc. The nodal structure of the particle and hole states around the Fermi surface is responsible for the multipole strength distribution of low energy particle-hole excitations. The figure shows that the states with low orbital angular momentum are much influenced by the boson-fermion interaction, while those with high angular momentum are almost insensitive to the values of $h=g$. This is because the additional fermion potential due to the boson-fermion interaction vanishes outside the boson density distribution. For instance, since the yrast single particle wave functions with angular momentum l are peaked around $r \approx R_B$, those fermion states with $l > (R_B/\lambda)^2$, R_B being a typical edge radius of the boson distribution, would not be much influenced by the boson-fermion interaction. (In the present case $R_B \approx 3$, and the above relation gives $l > 9$.)

C. Energy weighted moments and comparison with the sum rule calculation

RPA calculation provides approximate eigenvalues and wave functions for all the individual eigenstates and is useful to study details of the dynamics of the system. If one is interested in the gross behavior of the strength distribution or an approximate frequency of

the oscillation, one may rather consider the p -th energy weighted moments of the strength distribution,

$$m_p(L; \omega) = \sum_j (\hbar \omega_j)^p \langle 0 | F_L | j \rangle \langle j | F_L | 0 \rangle; \quad (32)$$

where $\hbar \omega_j$ is the excitation energy of the state $|j\rangle$. These moments can be expressed as ground-state expectation values of multiple commutators of F_L with the Hamiltonian [29,30]. It is known that this relation, sum rule, is conserved in RPA for some of the moments, i.e., the sum in the r.h.s. of Eq. (32) obtained from RPA eigenstates coincides with the expectation value of the commutator in the HF ground state [28,29]. Thus a comparison of the two would provide a criterion on the consistency of the RPA calculation. In particular, the first moment (energy weighted sum, EWS) m_1 is calculated from the double commutator of F_L and the Hamiltonian as

$$m_1(L; \omega) = \frac{1}{2} \langle 0 | [F_L, [\hat{H}, F_L]] | 0 \rangle; \quad (33)$$

where $\langle 0 |$ denotes a ground state expectation value [29]. We have checked that the sum rule is satisfied within 1% for all the multipole modes.

One can estimate the average frequency of the collective oscillation based on sum rules. There are several ways to define the average frequency depending on which part of the strength distribution is emphasized. In Ref. [18] the ratio of the third and the first moments

$$\omega = \frac{m_3}{m_1} \quad (34)$$

was studied based on sum rules. This definition is advantageous as it can be used to test the validity of the RPA calculation as mentioned earlier. In later discussions we consider also the average frequency calculated by

$$\omega_{av} = \frac{m_1}{m_0} \quad (35)$$

which has more weight in the low-frequency strength compared with ω . The two frequencies should coincide when a single collective state exhausts the strength. We discuss later also the width of the strength distribution defined by

$$= \frac{m_2}{m_0} \frac{m_1}{m_0} 2^{\#_{1=2}} : \quad (36)$$

In Fig. 2 we show the average frequency Eq. (34) for $L = 0, 1, 2$ and $\epsilon = +$; given by the sum rule (33) and the one directly calculated in RPA. We find a good agreement of the two calculations in a wide range of the bose-fermi interaction parameter h for a fixed g . There is a discrepancy at very large values of $|h|$, especially in the strongly attractive case. In the latter case, an induced instability of the ground state due to the bose-fermi attraction may be close [16], which suggests that a larger configuration space may be required to satisfy the sum rule. In fact, by increasing the number of particle-hole states, we obtained a better agreement.

D. Distribution of multipole strengths

Now we show the distributions of the multipole strengths. Figures 3, 7, 10, 11 respectively show the strength distributions for $L = 0, 1, 2$ and 3, for either the fermionic/bosonic or the in-phase/out-of-phase operators.

1. monopole

In Fig. 3 we show the monopole strength distribution, $|F_0|^2$ against ω , for $\epsilon = f; b$ and for three values of $h=g$. Here one expects a volume oscillation of boson and/or fermion densities. For $h = 0$ and for a large number of particles, the bosonic monopole oscillation will be located around $\frac{p}{5}\omega_0$ as given by the collisionless hydrodynamics [2, 21], while the fermionic one is concentrated at $2\omega_0$. The latter property is due to the almost degenerate values of the relevant particle-hole energies contributing to the monopole oscillation. The present calculation shows that this situation persists even for large values of $h=g$, although the bosonic frequency is slightly shifted. The fermionic strength is distributed over a few states around $2\omega_0$, showing that the induced fermi-fermi interaction via bosons is not strong enough to make a coherent superposition of the fermion particle-hole states. The total

monopole strength for fermion is by an order of magnitude larger than that for boson, even though the number of fermions involved in the excitation is smaller because of the Pauli principle, e.g. $m_1 = 2590\hbar_0^{-4}$ for fermion and $m_1 = 419\hbar_0^{-4}$ for boson at $h=g=1$. This is because of the broader density distribution for fermions.

The strength distribution may suggest that the fermions and bosons are moving independently even for rather large values of $h=g$. This is not necessarily the case, however, as one may see in Fig. 4, where we plot the dynamical structure factor for the three cases, i.e., the states at $\omega_0 = 2.03$ for $h=g=5.0$, at 2.01 for $h=g=1.0$ and at 1.98 for $h=g=-3.0$, which carry the largest strengths for the in-phase monopole operator. Although the fermionic strength is far larger than the bosonic one for this state, the mixture of the bosonic component is not small and is peaked at larger values of the momentum transfer q as shown by the dashed lines. The latter shows that the bosons oscillate in the inner region although not quite recognizable as far as one studies only the F_0 distribution.

In Refs. [16,18] we suggested that an instability towards collapse may occur at large negative values of $h=g$ and may be signaled by the lowering of ω_0 . In the present calculation with smaller number of particles this is not apparent in Fig. 2. In Fig. 5 we show the strength distribution at $h=g=-6.65$. This value is close to the critical value of instability around 6.7 estimated from the Møller's condition [7,16] and around 6.8 from the condition by Roth and Feldmeier [17]. We find a lowering of a single state which carries 13.9% of the EWS. The average frequency for this case is $\omega_0 = 1.92\hbar_0$ appreciably lower than the value $2\hbar_0$ for $h=g=-5$. At more negative values of $h=g$ we could not find a stable ground state.

Let us study the character of the low-lying excited states by considering the response to the probe

$$F(\theta) = F^+ \cos \theta + F^- \sin \theta \quad (37)$$

parametrized by θ . In Ref. [18] the angle θ was determined by minimizing the average frequency ω_0 for $F(\theta)$ so as to find the character of the probe which favors the low-lying

states. Once the value of the parameter, α_{in} is determined for a given $h=g$, one may consider an operator perpendicular to $F(\alpha_{\text{in}})$, i.e., $F_{\perp} = F^{\dagger} \sin \alpha_{\text{in}} - F \cos \alpha_{\text{in}}$, which may favor the high-lying state. Alternatively, one may maximize the EWS within the model space to determine the value α_{ax} of the operator to characterize the high-lying states. Figure 6 shows the strength distribution for these three types of operators at $h=g = 5.0$. The value $\alpha_{\text{in}} = 0.12$ suggests that, at this highly repulsive value of the interaction, a slightly in-phase type oscillation is favored in order to avoid an overlap of bosons and fermions, see the density distribution in Ref [7,8,13,17]. We note that the distribution for the perpendicular operator F_{\perp} is concentrated and is similar to the one for $F(\alpha_{\text{ax}})$. The latter, however, is an almost bosonic type operator and suggest that the strength distribution alone is not sufficient to characterize the structure of high-lying states. A similar study has been made for a very attractive case $h=g = -6.65$. In this case we obtain $\alpha_{\text{in}} = 0.01$, i.e., almost in-phase, and the strength distribution is similar to Fig. 5. Thus the in-phase character of the low-lying mode which favors the overlap of the two kinds of particles is clearly seen in the determination of $F(\alpha_{\text{in}})$.

2. dipole

Dipole strength distributions for the in-phase and the out-of-phase operators are shown in Fig. 7. The strong peak in the in-phase strength distribution corresponds to the center-of-mass oscillation of the whole system. For many-particle systems confined in a common oscillator potential the center-of-mass motion is decoupled from other (intrinsic) degrees of freedom of the system, resulting in the oscillation with the same frequency ω_0 . This relation can be represented by the commutation relation of the dipole operator and the Hamiltonian, and should hold also within RPA [28]. In the present numerical calculation, however, the state at $\omega = \omega_0$ does not exhaust the whole strength for the in-phase oscillation; the largest deviation occurs at $h=g = -1$ having 80% of the EWS. This is because the single-particle model space in our numerical calculation is not sufficient to completely decouple

the center of mass motion, especially at strong coupling cases where the deviation of the single particle potential from the oscillator becomes large. The m_1 sum rule is, nevertheless, almost satisfied as mentioned earlier, and is determined by the total number of boson and fermion particles, where the latter number is dependent on the value of $h=g$. Smaller value of the sum rule percentage at $h=g = 1$ is mainly due to the appearance of the almost degenerate state ($\omega = \omega_0 \sim 10^{-5}$) at this energy.

All other dipole oscillations should be orthogonal to the center-of-mass motion and thus are out-of-phase type in character. One may note that at repulsive values of h the dominant part of the out-of-phase strength is located below ω_0 , although the strength carried by each individual state is not very large. As discussed in Ref. [18], this may reflect the ground state density distribution which favors the out-of-phase oscillation by making the overlap of boson and fermion distributions smaller. Figure 8 shows transition densities for the out-of-phase type oscillations at $h=g = 5.0; 1.0; -3.0$ which carry the largest strengths; $\omega = \omega_0 = 0.700$ for $h=g = 5.0$, 0.956 for $h=g = 1.0$ and 1.14 for $h=g = -3.0$. Bosons and fermions move in the opposite directions so as to make the overlap smaller around the surface of the boson distribution. One can observe that the bosonic transition density is large and robust, while the fermionic one is feeble and is spread over the whole system. This situation may be analogous to the soft dipole mode speculated in neutron-rich nuclei wherein the protons oscillate almost free in the sea of neutrons [31]. Dynamical structure factors corresponding to these states are shown in Fig. 9. Here the bosonic and the fermionic responses are shown together with the one for a hypothetical out-of-phase type probe. By changing the momentum transfer one would find a structure corresponding to the oscillation of the two kinds of particles.

It was suggested in [7,19] that for a very strong repulsion between bosons and fermions with sufficient number of particles, the system may become unstable towards a phase separation of the two kinds of particles. Out-of-phase dipole strength distribution in Fig. 7 indeed shows a softening of the strength distribution at large value of $h=g$. We cannot conclude from the present calculation, however, if this tendency is related to the mentioned instability.

3. quadrupole

One finds from the quadrupole strength distribution in Fig. 10 that the fermionic strength is split into low- and high-energy parts, while the bosonic one is concentrated. The higher strengths for the fermions are due to the $2h!_0$ excitation of the particle from the occupied single-particle states and are similar in character to the bosonic excitation. In contrast, the lower fermion strengths come from the matrix elements of the quadrupole operator F_2 which re-orient the single particle states within the same oscillator shell of $N = 2n + 1$ around the Fermi surface. This transition normally involves a change of nodes by one, see Fig. 1, and the corresponding strengths are smaller than the higher ones. One may note that the quadrupole bosonic strength is located slightly higher than $\frac{P}{2!}_0$ as expected for the collective oscillation in the large N limit [2], which may be due to a rather small number of particles in the present calculation.

We note that the strength distribution tends to be fragmented at large (repulsive) value of the interaction parameter $h=g$ as seen in Fig. 10. This is because the average potential deviates appreciably from the harmonic oscillator potential, giving rise to a dispersion in the fermion particle-hole energies, see Fig. 1. Strong fermion-boson interaction would then be responsible to scatter the bosonic strengths, too.

4. octupole

Octupole strength distribution is shown in Fig. 11. Here again the fermionic strength is split into $h!_0$ and $3h!_0$ regions due to the character of the multipole operator F_3 . We note also that the frequency of the bosonic oscillation is much larger than the hydrodynamic value $\frac{P}{3!}_0$ [21].

We find a striking change in the fermionic strength distributions depending on the sign of the bose-fermi interaction. While for a strongly repulsive case ($h=g = 5.0$) the region between the low- and high-lying states is almost filled up by small strengths, the one for a

strongly attractive case ($h=g = -3/0$) shows a large gap in the strength distribution. This may be traced back to the structure of the single-particle states in Fig.1. The large strengths around $3!_0$ are due to high orbital angular momentum states with $l_p = l_h = 3$ which stay robust against $h=g$ as discussed earlier. Smaller strengths due to low l_p and l_h states are, on the other hand, sensitive to the interaction, and the corresponding particle-hole energies are below (for $h=g > 0$) or above (for $h=g < 0$) the unperturbed value $3!_0$. This may be understood by noting that the particles passing through the center (small l orbit) feel the shallow (for $h=g > 0$) or deep (for $h=g < 0$) potentials and are thus more easy or hard to excite. For the strengths around $!_0$ different combinations of orbits are involved, and the strengths are broadened by the deviation from the oscillator potential.

E. Time evolution

To study the collective oscillation of the cold atomic gases, the current experiments on BEC exert a time-dependent field on the system and then observe the time development of the shape and the size of the condensate [1]. This procedure generally excites a number of normal modes, and one may in principle be able to resolve each mode by performing Fourier transform as far as the time duration is long enough. To simulate the situation we consider a time evolution of the system after one applies an external weak pulse of the step-function type, i.e., $V = F_0$ for $t = t_0$. The calculation is performed within the lowest order perturbation theory. (t is chosen as $t = 10^{-2}!_0^{-1}$.)

1. monopole

First we consider a perturbation of monopole type

$$V = m!_0! \frac{p}{4} F_0 \quad (38)$$

with $! = !_0$ which is applied to the ground state of the system for a short period t . The effective frequency of the external oscillator potential for fermions and/or bosons is then

changed into σ_0 depending on the choice of σ . Time dependence of the rms radius of bosons and fermions is plotted in Fig. 12 at $h=g=3$ for the fermionic external field, $\sigma = f$. Frequency of the short period oscillation is related to the average frequency of the strength distribution, e.g., $\omega_{av} = 1.99\omega_0$. That of the long period one, on the other hand, reflects the width of the distribution. For instance, the slow decrease of the envelope for $q \rightarrow \infty$ $h r_f^2 i$ would imply a very narrow width of the strength distribution. The bottom of Fig. 12 shows the Fourier transform of $h r_f^2 i(t) - h r_f^2 i_0$ which recovers the sharp peak structure of the strength distribution in Fig. 3. Time evolution of the bosonic radius shows a rather regular modulation, and its beat frequency is estimated about $0.125\omega_0$, which is consistent with the halfwidth $\Delta = 0.127\omega_0$.

2. dipole

For the dipole case we take the perturbing potential

$$V = m \omega_0^2 z \sqrt{\frac{4}{3}} F_1; \quad (39)$$

where $z(\tau)$ measures the shift of the centers of the oscillator potentials felt by fermions and/or bosons. In Fig. 13 we show the time dependence of the center-of-masses of bosons and fermions for the out-of-phase external dipole impulse, $\sigma = f$, at $h=g=5$. The frequency of the oscillation is consistent with the average frequency $0.90\omega_0$ for the dipole strength distribution. The amplitude of the oscillation shows an irregular behavior, suggesting that the strength distribution does not have a simple structure. The lowest part of the figure shows the Fourier transform of the relative distance of the fermion and boson center-of-mass positions, $N_f h z_f i - N_b h z_b i$, which is sufficient to recover the behavior of the original strength distribution given in Fig. 7.

IV . S U M M A R Y A N D C O N C L U S I O N

In the present paper we performed an RPA calculation of the polarized bose-fermion mixed system of alkali metal gases at zero temperature. We solved a coupled Gross-Pitaevskii-Thomson-Fermi equations to obtain the ground state for several values of the boson-fermion interaction strength with a fixed value of the boson-boson interaction. Single particle states of bose and fermi particles are calculated based on the mean field produced by the obtained ground state density. The density distribution constructed from the occupied single-particle orbits agrees well with the original one, suggesting the self-consistency of the calculation. We calculated and diagonalized the RPA matrix to obtain excitation energies and wave functions for multipoles $L = 0;1;2;3$. We then calculated strength distributions for bosonic/fermionic and in-phase/out-of-phase multipole operators, and also transition densities and dynamical structure factors for some of the collective states.

We first calculated energy weighted moments of the strengths to study average behavior of the strength distribution. Comparison of the first moments with the sum rule predictions for $L = 0;1;2$ shows that the RPA configuration space is sufficient to within 1%. A glance at the monopole distribution suggests that fermions and bosons are moving rather independently for the adopted parameters, which turns out not to be the case if we study the dynamical structure factors. We find, in fact, that the long wavelength oscillation of fermions in the surface is coupled to the internal short-wavelength oscillation of bosons. For a strong attractive boson-fermion interaction, the calculation suggests a softening of in-phase monopole oscillation. We studied also the structure of the low-lying out-of-phase type dipole modes. Lowering of the energy is related to the ground state density distribution of bosons and fermions which favors the out-of-phase oscillation. Transition densities for these modes suggest that the bosons oscillate on their way through the cloud of fermions, which is analogous to the soft dipole mode discussed in neutron-rich nuclei. We also calculated the strength distributions for quadrupole and octupole modes, and studied, in particular, the origin of the fragmentation of fermionic strengths. Finally we considered time dependent

behavior of the trapped bose-fermi system after an impulse of a multipole external field. By Fourier transforming the time-dependent oscillating behavior of the system, we could recover the gross structure of the strength distribution.

REFERENCES

- [1] M . H . Anderson, J . R . Ensher, M . R . Matthews, C . E . Wieman and E . A . Cornell, *Science* 269, 198 (1995); K . B . Davis, M . -O . M ewes, M . R . Andrews, N . J . van D ruten, D . S . Durfee, D . M . Kum and W . K etterle, *Phys. Rev. Lett.* 75, 3969 (1995).
- [2] F . Dalfovo, S . Giorgini, L . P . P itaevskii and S . Stringari, *Rev. M od. Phys.* 71, 463 (1999).
- [3] D . S . Jin, J . R . Ensher, M . R . Matthews, C . E . Wieman, and E . A . Cornell, *Phys. Rev. Lett.* 77, 420 (1996); M . -O . M ewes, M . R . Andrews, N . J . van D ruten, D . M . Kum, D . S . Durfee, C . G . Townsend, and W . K etterle, *Phys. Rev. Lett.* 77, 988 (1996).
- [4] B . D eM arco and D . S . Jin, *Phys. Rev. A* 58, 4267 (1998); *Science* 285, 1703 (1999); B . D eM arco, S . B . Papp and D . S . Jin, *Phys. Rev. Lett.* 86, 5409 (2001).
- [5] A . G . Truscott, K . E . Strecker, W . I . M cA lexander, G . B . Partridge and R . G . Hulet, *Science* 291, 2570 (2001).
- [6] F . Schreck, L . Khaykovich, K . L . Corwin, G . Ferrari, T . Bourdel, J . Cubizolles, and C . Salomon, *Phys. Rev. Lett.* 87, 080403 (2001).
- [7] K . M oller, *Phys. Rev. Lett.* 80, 1804 (1998).
- [8] M . Am oruso, A . M inguzzi, S . Stringari, M . P . Tosi and L . V ichi, *Eur. Phys. J. D* 4, 261 (1998).
- [9] T . M iyakawa, K . O da, T . Suzuki and H . Yabu, *J. Phys. Soc. Japan* 69, 2779 (2000).
- [10] M . J . Bijlsma, B . A . H eringa and H . T . C . Stoof, *Phys. Rev. A* 61, 053601 (2000).
- [11] L . V ichi, M . Inguscio, S . Stringari, and G . M T ino, *Eur. Phys. J. D* 11, 335 (2000).
- [12] L . V ichi, M . Inguscio, S . Stringari and G . M T ino, *J. Phys. B : At. M ol. Opt. Phys.* 31 L899 (1998).

- [13] N . Nygaard and K . M . Iner, Phys. Rev. A 59, 2974 (1999).
- [14] X . X . Yi and C . P . Sun, Phys. Rev. A 64, 043608 (2001).
- [15] L . V iverit, C . J . P ethick and H . Sm ith, Phys. Rev. A 61, 053605 (2000).
- [16] T . M iyakawa, T . Suzuki and H . Yabu, Phys. Rev. A 64, 033611 (2001).
- [17] R . Roth and H . Feldm eier, Phys. Rev. A 65, 021603(R) (2002).
- [18] T . M iyakawa, T . Suzuki and H . Yabu, Phys. Rev. A 62, 063613 (2000).
- [19] A . M inguzzi and M . P . Tosi, Phys. Lett. A 268, 142 (2000).
- [20] P . Capuzzi and E . S . Hernandez, Phys. Rev. A 64, 043607 (2001).
- [21] S . Stringari, Phys. Rev. Lett. 77, 2360 (1996).
- [22] J . Stenger, S . Inouye, A . P . Chikkatur, D . M . Stam per-K um, D . E . P ritchard, and W . K etterle, Phys. Rev. Lett. 82, 4569 (1999); D . M . Stam per-K um, A . P . Chikkatur, A . G orlitz, S . Inouye, S . G upta, D . E . P ritchard, and W . K etterle, Phys. Rev. Lett. 83, 2876 (1999).
- [23] F . Zam belli, L . P itaevskii, D . M . Stam per-K um, and S . Stringari, Phys. Rev. A 61, 063608 (2000); A . B runello, F . D alfovo, L . P itaevskii, S . Stringari, and F . Zam belli, Phys. Rev. A 64, 063614 (2001).
- [24] P . R ing and P . Schuck, The Nuclear M any-B ody P roblem (Springer-Verlag, New York, 1980).
- [25] F . E . Serr, T . S . D um itrescu, T . Suzuki and C . H . D asso, Nucl. Phys. A 404, 359 (1983).
- [26] R . C ote, A . D algamo, H . W ang and W . C . Stwalley, Phys. Rev. A 57, R4118 (1998).
- [27] L . D . Landau and E . M . L ifshitz, Q uantum M echanics N on-Relativistic Theory 3rd ed. (Butterworth-Heinem ann, O xford, 1981).

- [28] D . Thouless, Nucl. Phys. 22, 78 (1961).
- [29] O . Bohigas, A . M . Lane and J. M artorell, Phys. Rep. 51, 267 (1979).
- [30] E . Lipparini and S. Stringari, Phys. Rep. 175, 103 (1989).
- [31] K . Ikeda, Nucl. Phys. A 538, 355c (1992).

FIGURES

FIG .1. Fermion single particle energies for $h=g = 5.0; 1.0; -3.0$ against orbital angular momentum quantum number. Energies are measured from the Fermi energy. Eigenstates which are degenerate at $h=g = 0$ are connected by solid lines.

FIG .2. Average frequencies of the collective excitations in the sum rule formalism. Average frequencies ω , Eq. (34), in units of ω_0 is plotted against interaction strength ratio $h=g$ with fixed g . Solid and dotted lines respectively show the in- and out-of-phase oscillations. For a comparison, average frequencies calculated from the ground state expectation values of double commutators, see Ref. [18], are plotted by dashed (in-phase) and dot-dashed (out-of-phase) lines.

FIG .3. Monopole strength distribution for fermionic and bosonic operators, F_0^f and F_0^b , at $h=g = 5.0, 1.0$ and -3.0 . Strengths in units of ω_0^4 are plotted against excitation energy.

FIG .4. Dynamical structure factors for the states in which in-phase monopole strengths are the largest. These states correspond to the ones at $\omega_0 = 2.03$ for $h=g = 5.0$, at 2.01 for $h=g = 1.0$ and at 1.98 for $h=g = -3.0$. Dotted and dashed lines correspond to the fermion and boson transition densities, F_0^{fb} , while solid lines are for the in-phase one, $F_0^+ = F_0^f + F_0^b$. The abscissa is $q = \hbar$, where q denotes the momentum transferred to the system by external probes.

FIG .5. Strength distribution for the in-phase monopole operator F_0^+ at $h=g = -6.65$ plotted against ω_0 .

FIG .6. Strength distribution for the ω -dependent monopole operator $F_0(\omega)$ at $h=g = 5.0$. Upper figure shows the strength distribution for the operator $F(\omega_{\min} = 0.12)$ which was determined so as to minimize the average frequency ω . Middle figure is the one for the operator $F_{\perp} = F(\omega = 0.38)$ which is perpendicular to the above operator. Lower figure is the strength distribution for the operator $F(\omega_{\max} = 0.27)$ which was determined to maximize the average energy.

FIG .7. Dipole strength distribution for in- and out-of-phase operators, F_1^+ and F_1^- . Strengths are measured in units of \hbar^2 .

FIG .8. Transition densities for the dipole oscillations with largest strengths of the out-of-phase type. Excitation energies of these states are $\omega_0 = 0.700$ for $h=g = 5.0$, 0.956 for $h=g = 1.0$ and 1.14 for $h=g = -3.0$. Solid and dotted lines respectively show the fermionic and bosonic transition densities, ρ_1^{fb} , in units of \hbar^3 .

FIG .9. Dynamical structure factors for the same states as given in Fig. 8. Dotted and dashed lines are those for the fermionic and bosonic transition densities while solid lines are those for the out-of-phase one, $S_1 = S_1^f + S_1^b$.

FIG .10. Quadrupole strength distributions for fermionic and bosonic operators, F_2^f and F_2^b , at $h=g = 5.0, 1.0$ and -3.0 .

FIG .11. Octupole strength distributions for fermionic and bosonic operators, F_3^f and F_3^b , at $h=g = 5.0, 1.0$ and -3.0 .

FIG .12. Time dependent oscillation of the bose-fermi system at $h=g = -3.0$ after an external impulse of fermionic monopole-type, Eq. (38). Time dependences of the root-mean-square radii (in units of \hbar) of fermions (upper figure) and of bosons (middle figure) are shown. Parameters of the impulse are: $\omega_0 = 0.01$ and $\omega_0 t = 0.01$. Differential equation in time is solved with the time mesh of $0.05\omega_0^{-1}$ up to $t_{max} = 100\omega_0^{-1}$. The lowest figure shows the Fourier transform (in an arbitrary unit) of the fermionic rms radius deviation from the ground state, $\langle r_f^2(t) \rangle - \langle r_f^2 \rangle_0$, which corresponds to the fermionic strength distribution given in Fig. 3 at $h=g = -3.0$.

FIG. 13. Time dependence of the oscillations of fermions and bosons at $\hbar=g = 5.0$ for an out-of-phase type external dipole impulse, Eq. (39). Upper and middle figures show the fermion and boson center-of-mass in the unit of ℓ_0 against elapsed time in the unit of ℓ_0^{-1} . Parameters are given by $z = 0.01$ and $\ell_0 t = 0.01$. Calculation is performed with time-mesh of $0.05\ell_0^{-1}$ and up to $t_{\text{max}} = 100\ell_0$. The lowest figure shows the Fourier transform (in an arbitrary unit) of the relative distance of fermions and bosons, $N_f \hbar z_f i - N_b \hbar z_b i$, with an energy resolution of 10^{-2} . The figure corresponds to the strength distribution of the out-of-phase type in Fig. 7 at $\hbar=g = 5.0$.

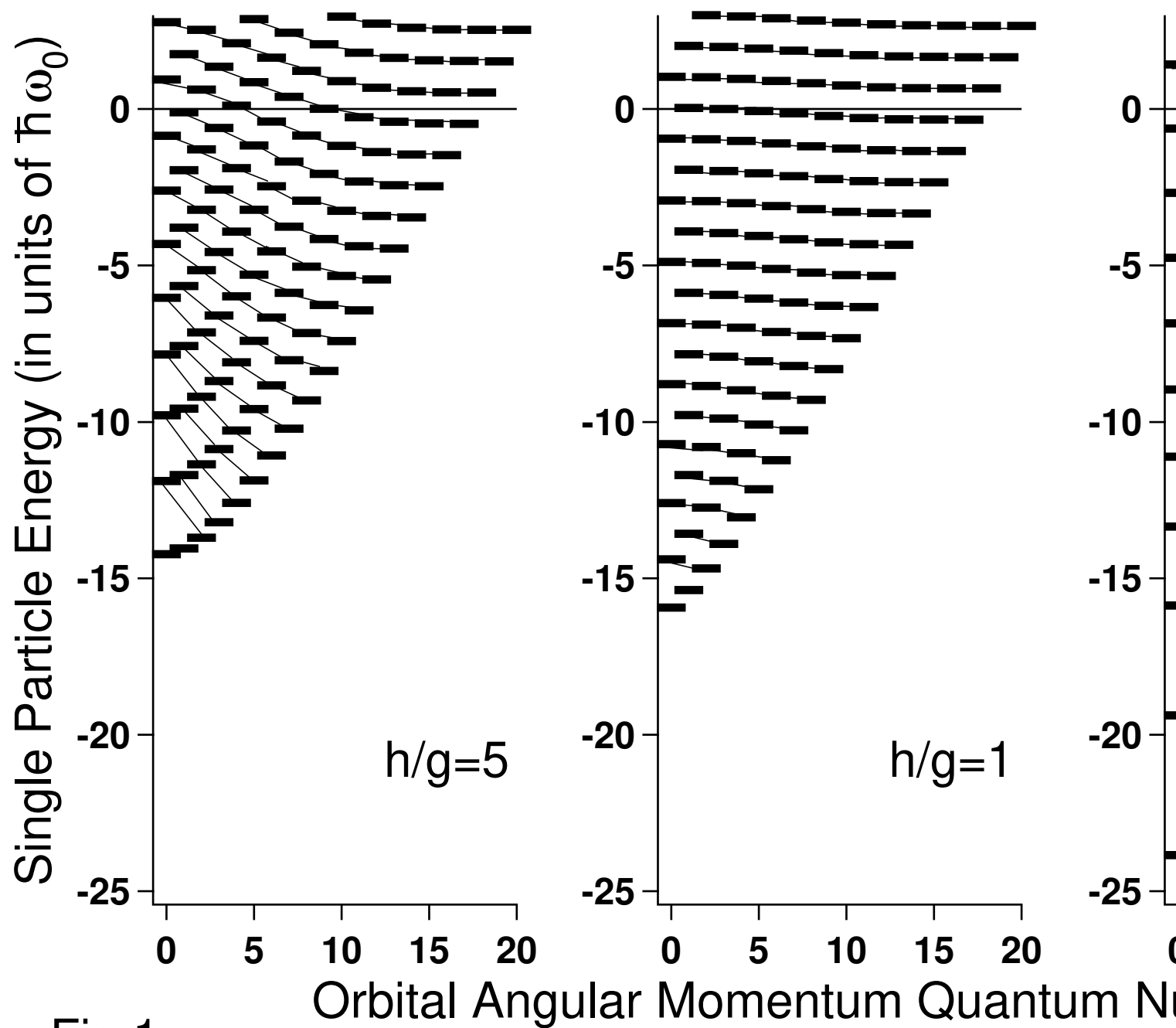


Fig.1

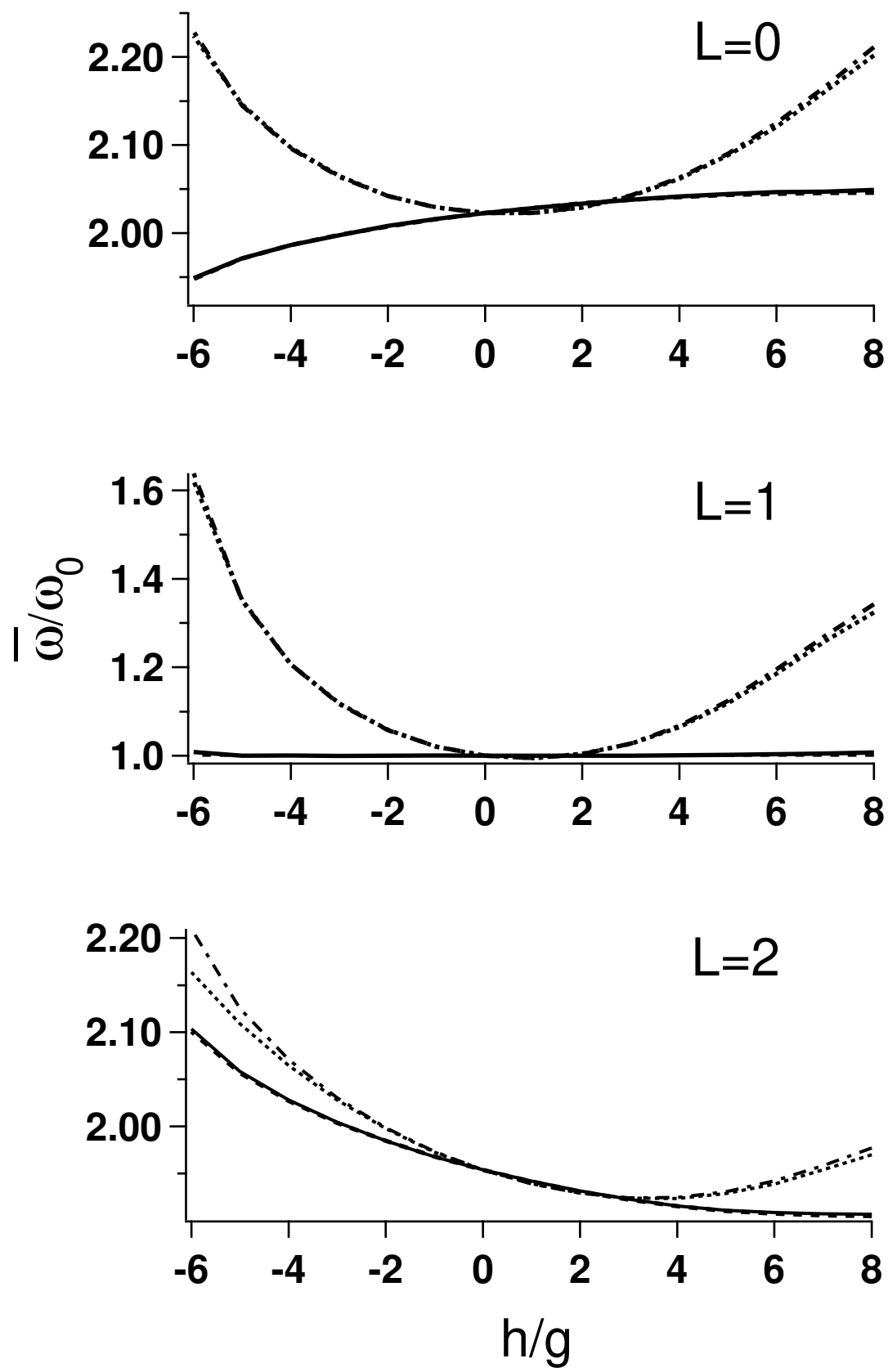


Fig.2

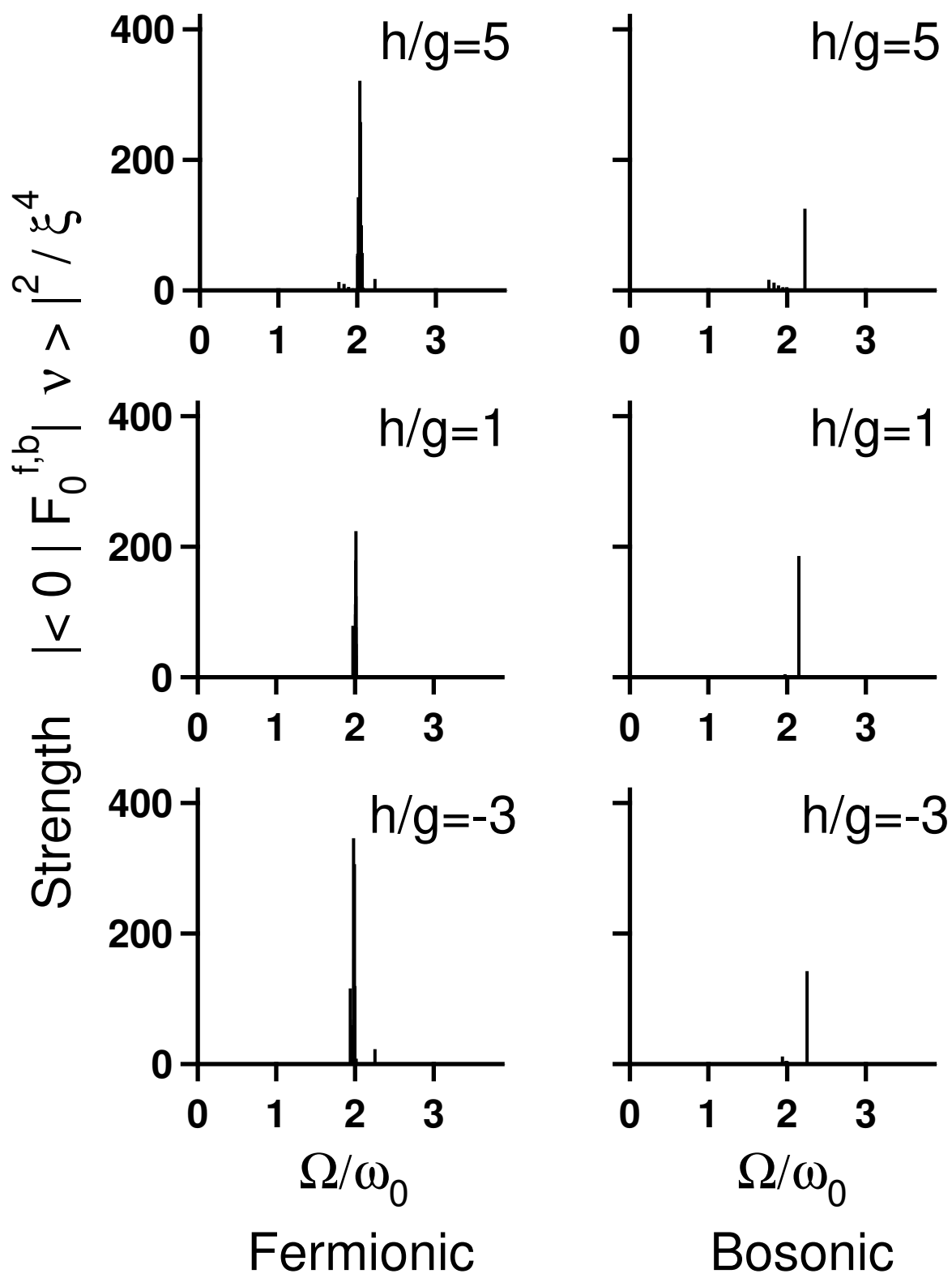


Fig.3

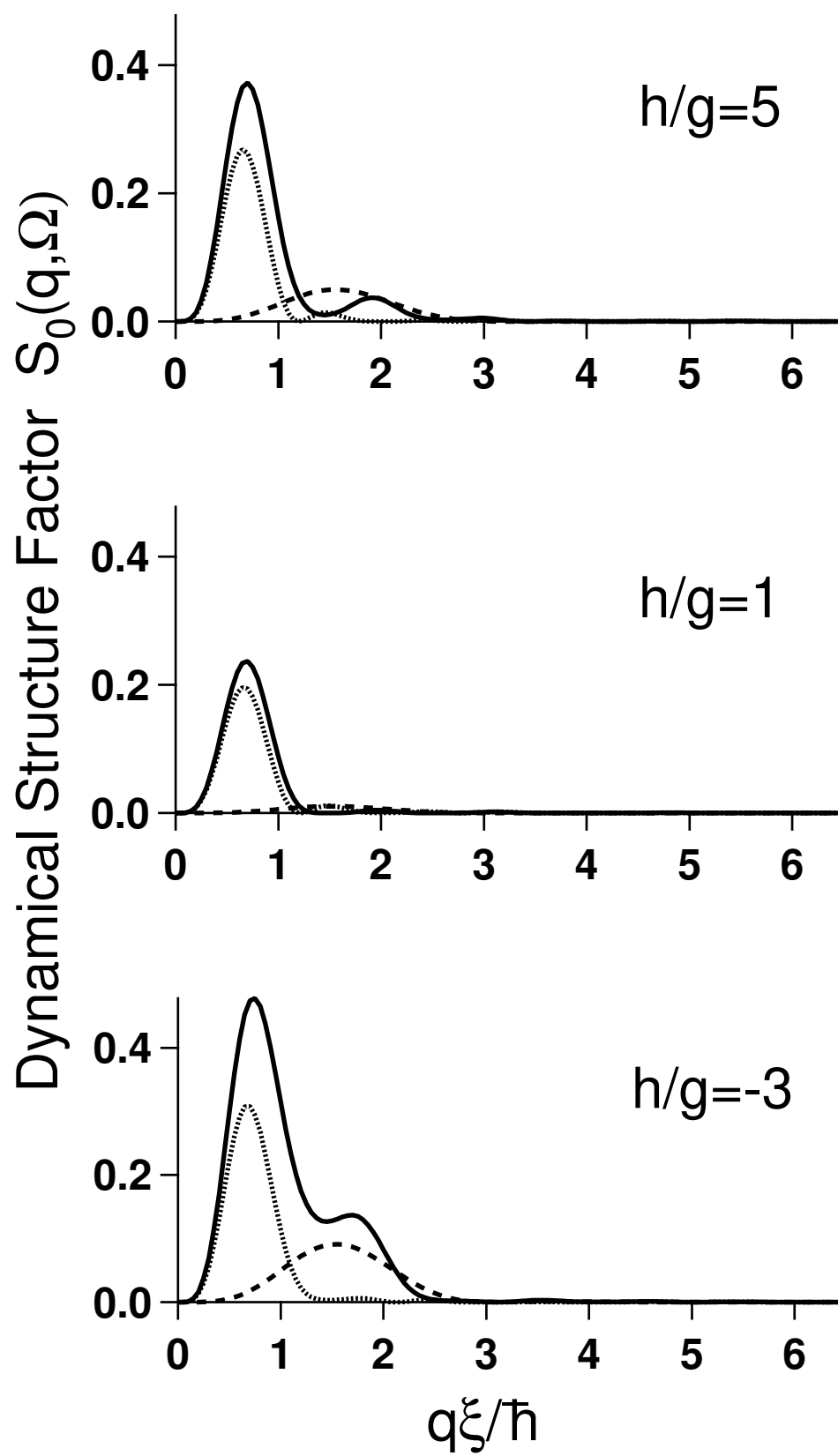


Fig.4

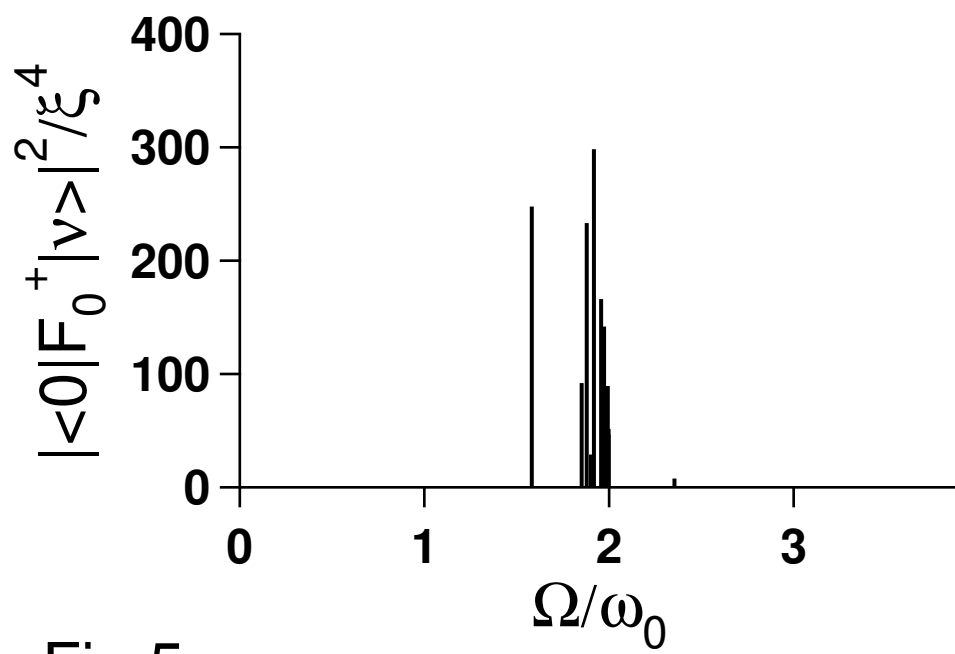


Fig.5

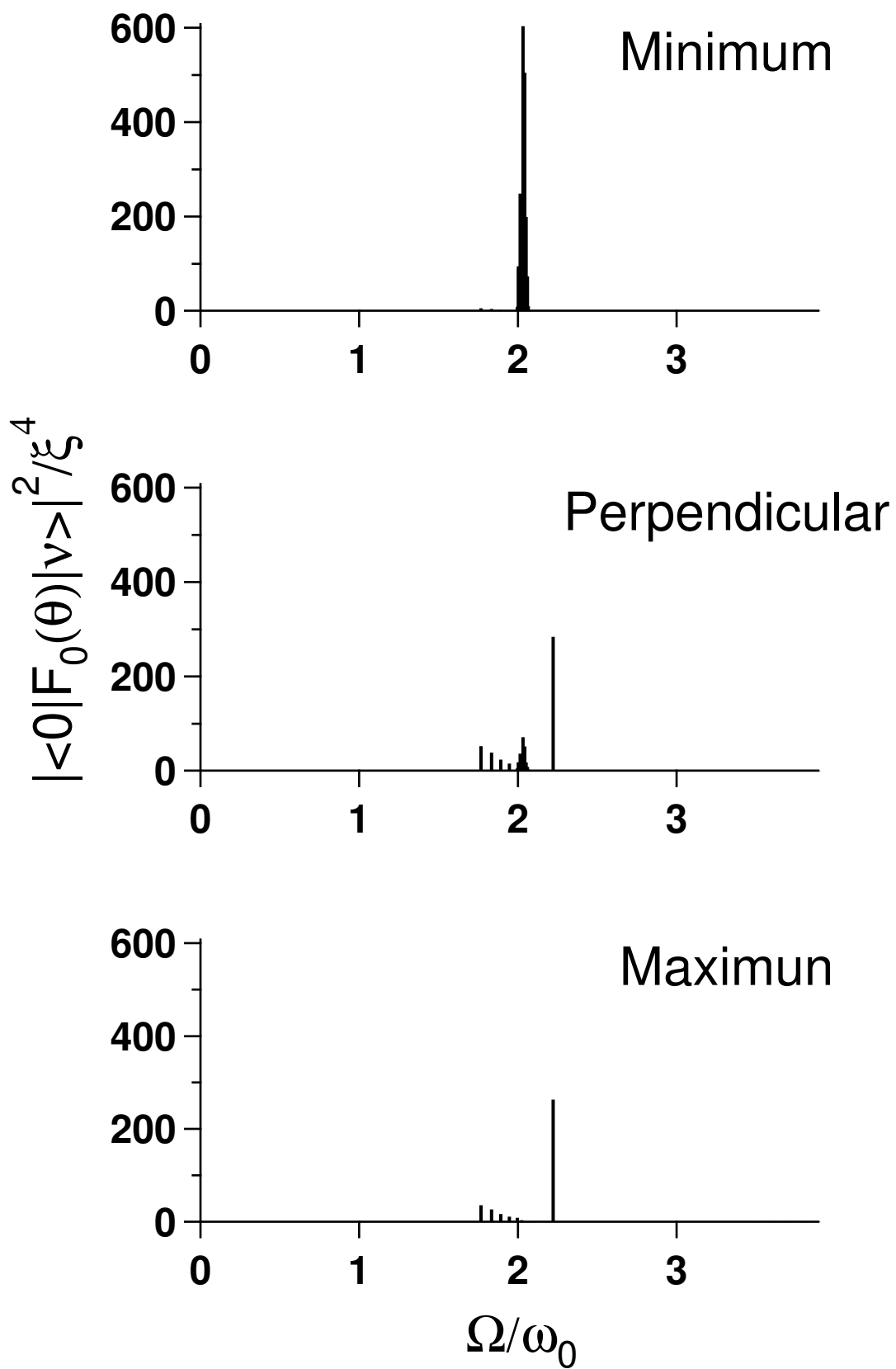


Fig.6

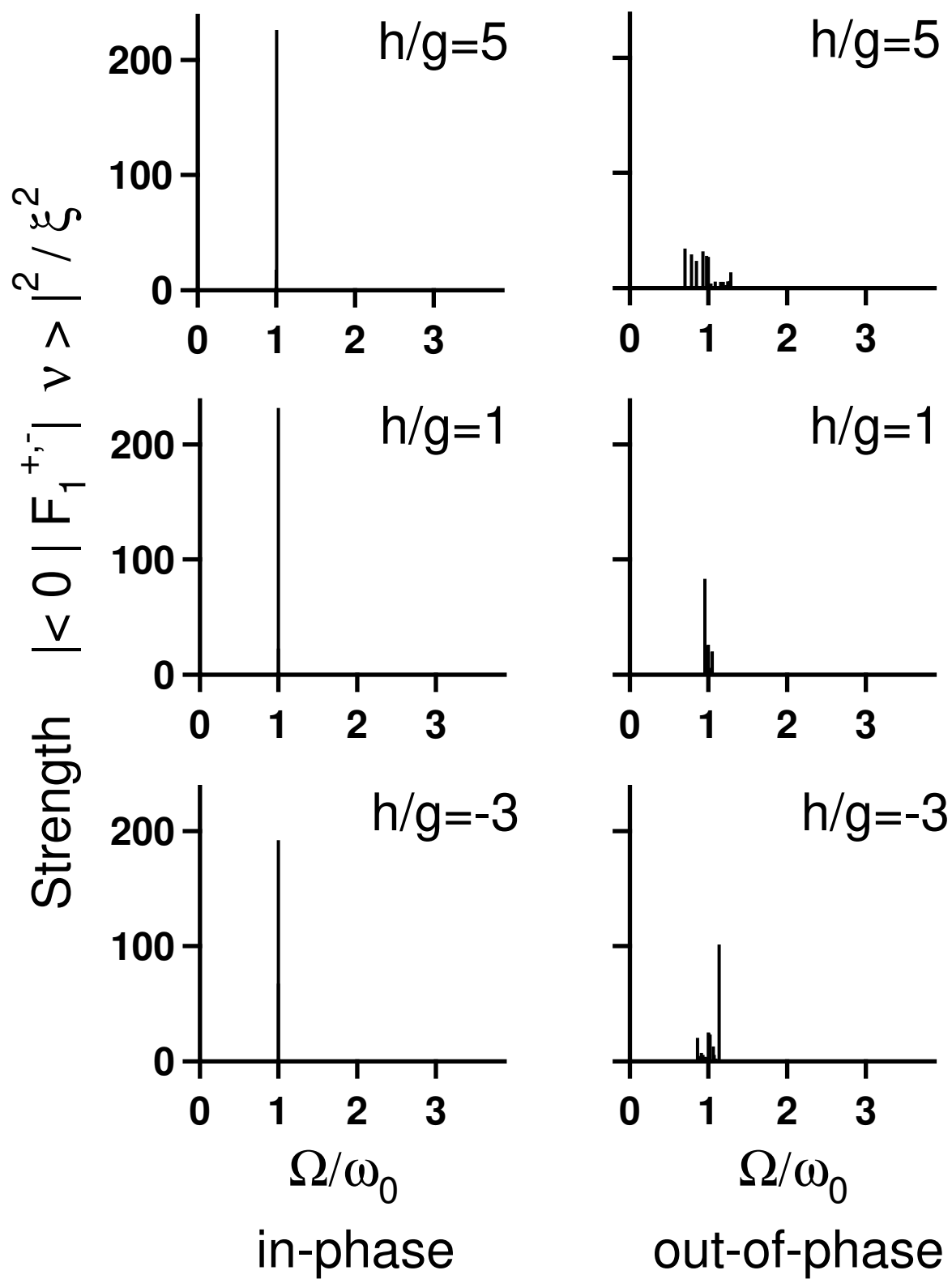


Fig.7

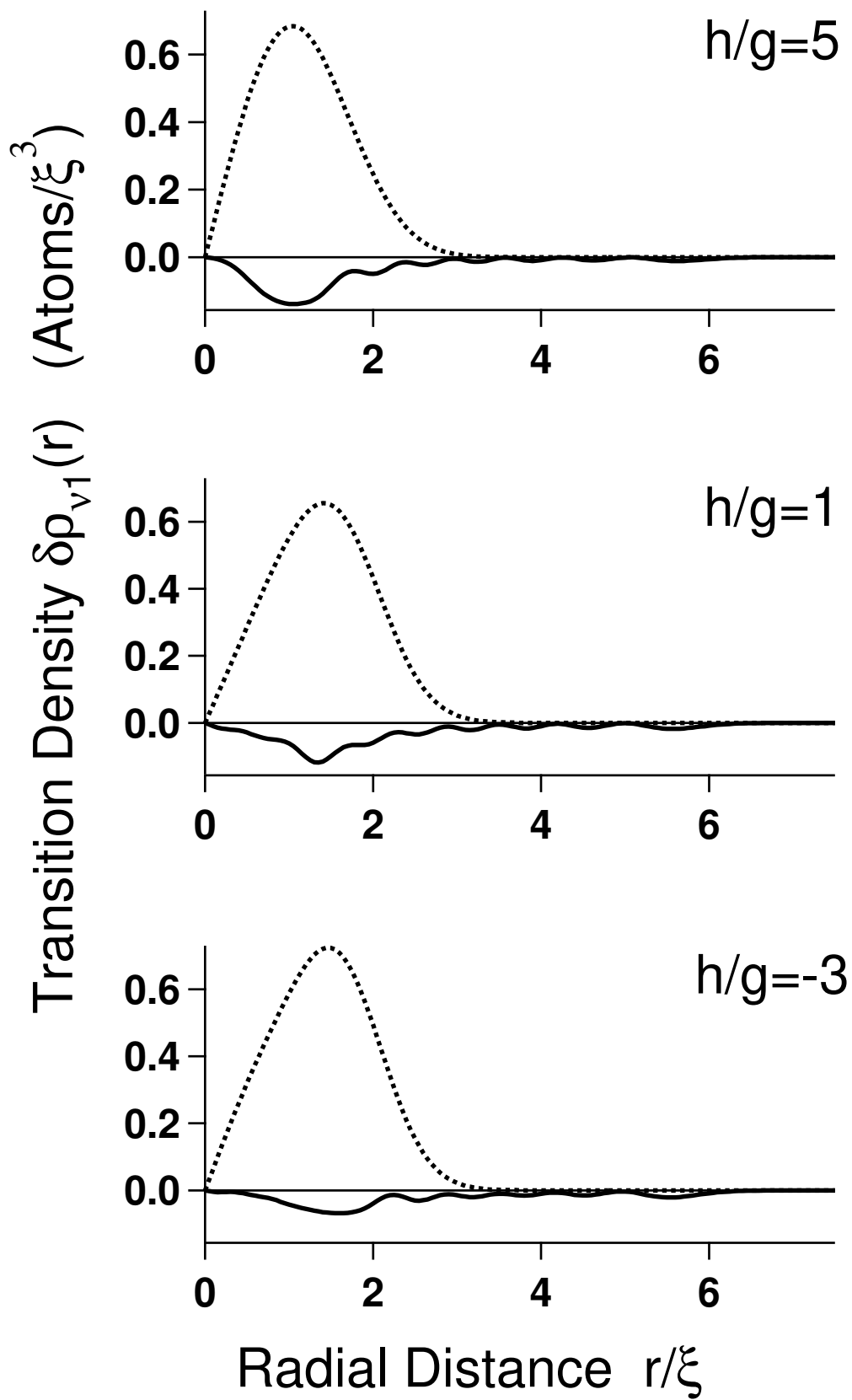


Fig.8

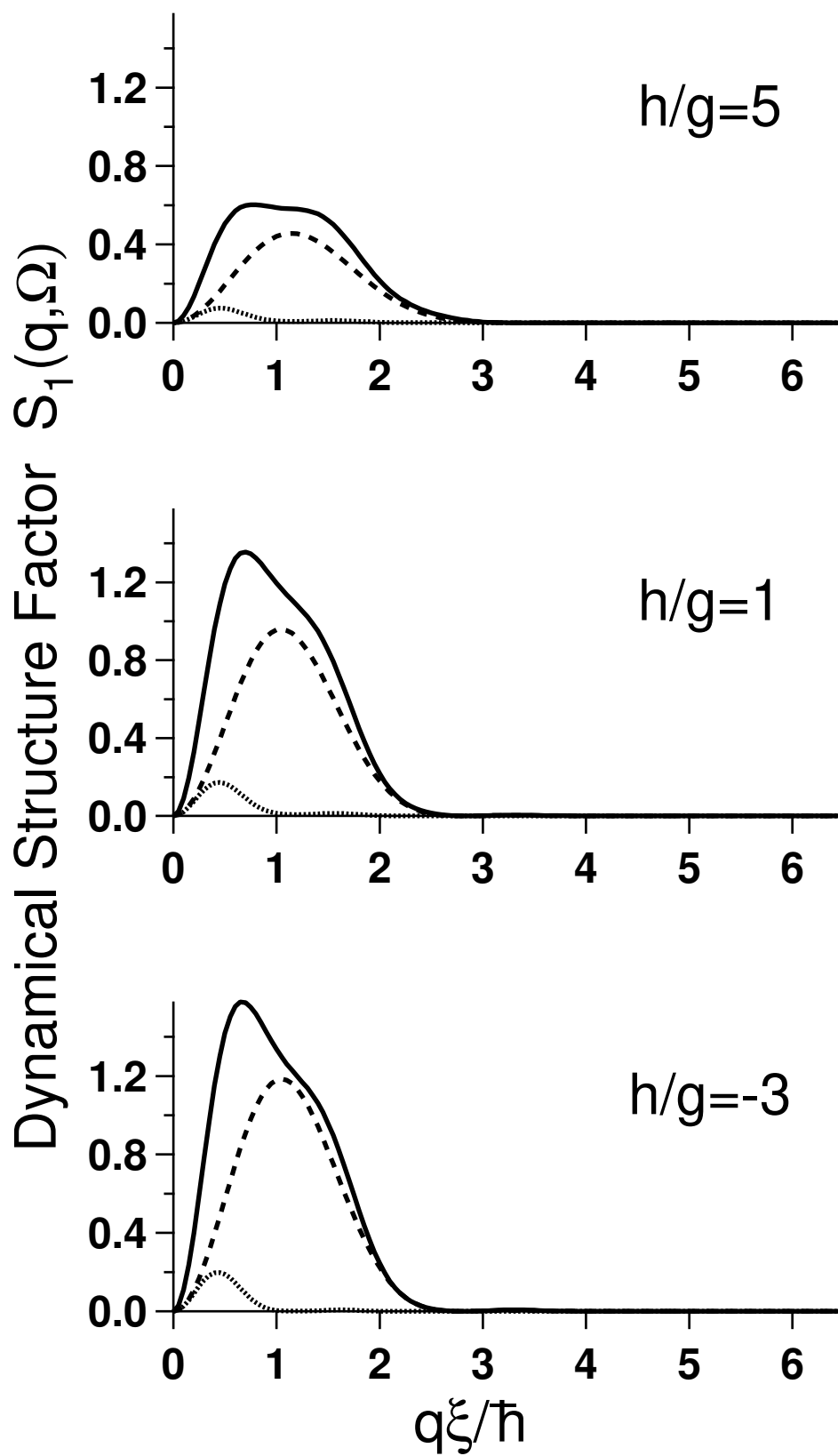


Fig.9

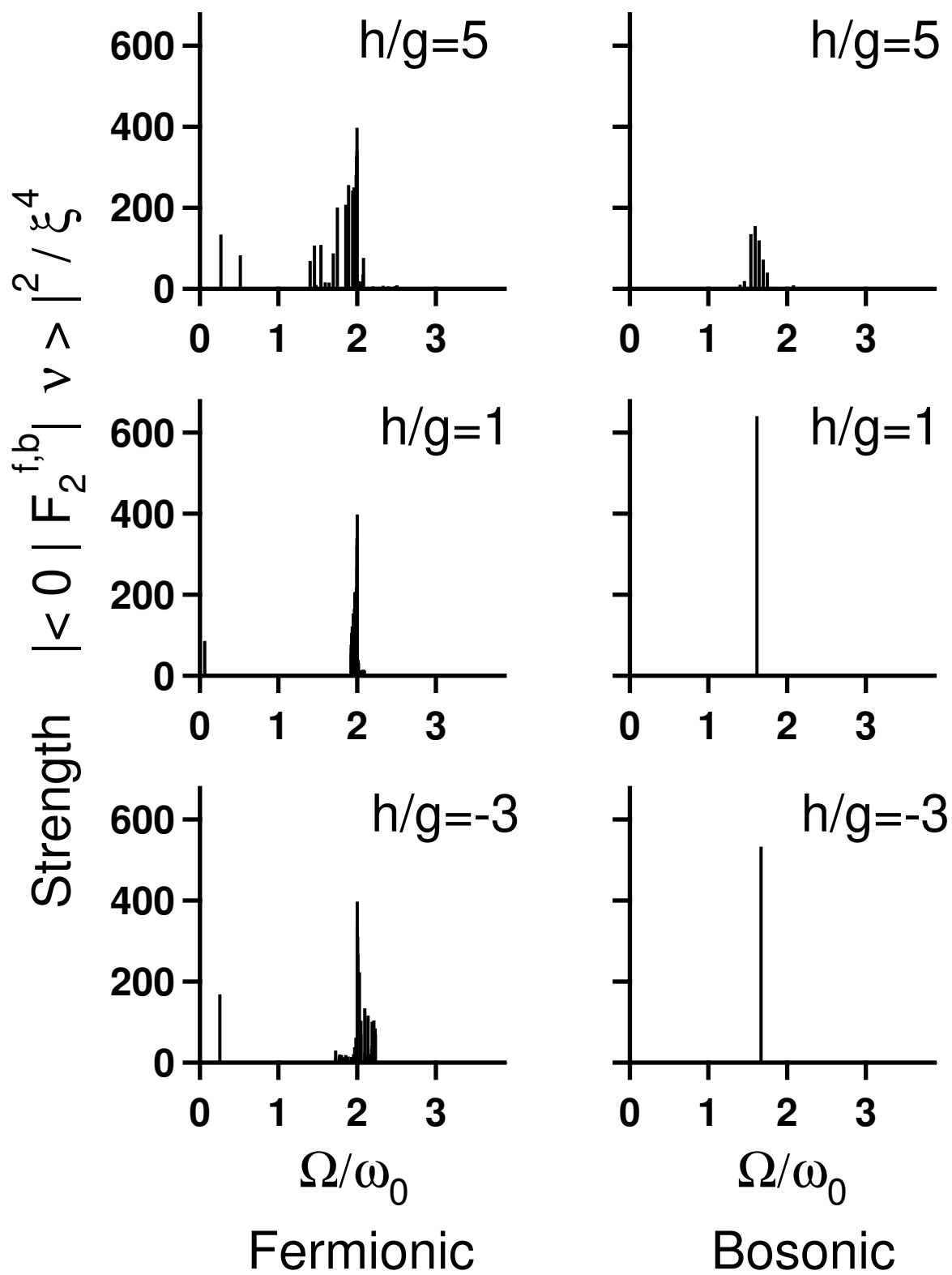


Fig.10

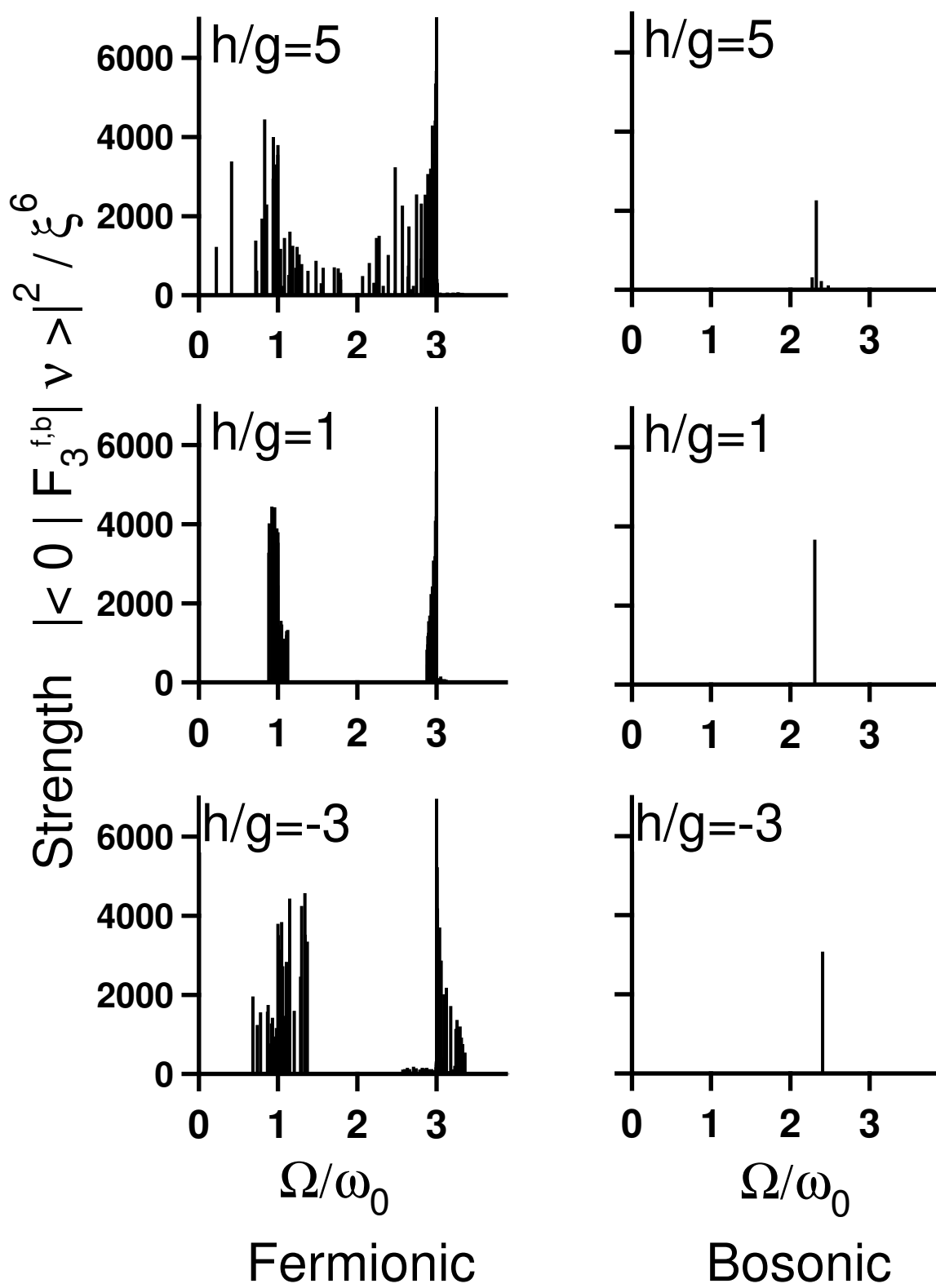


Fig.11

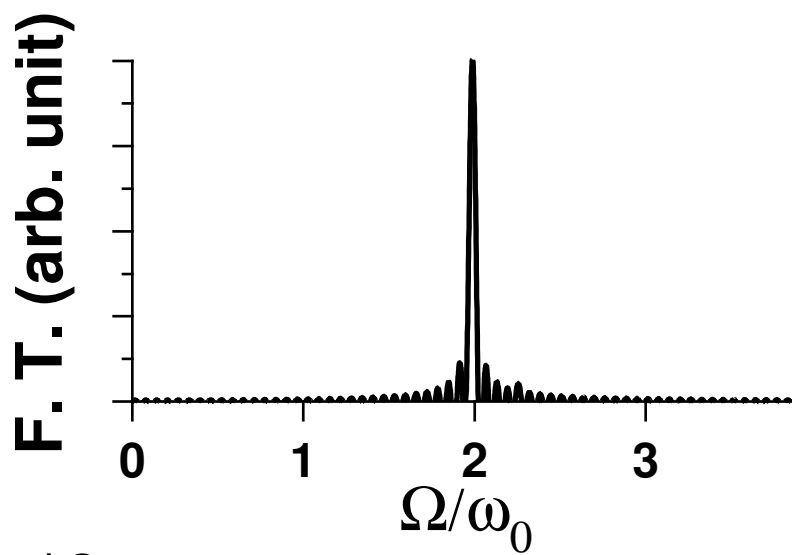
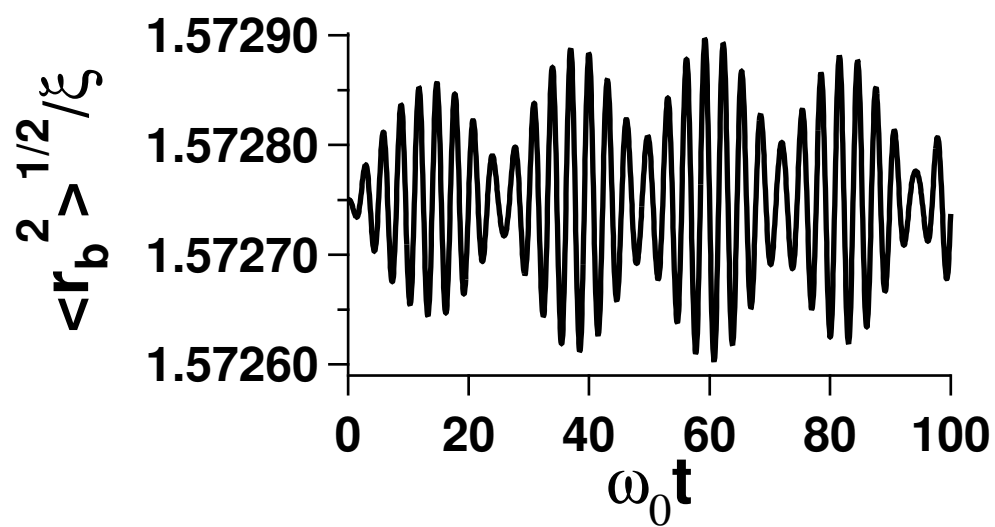
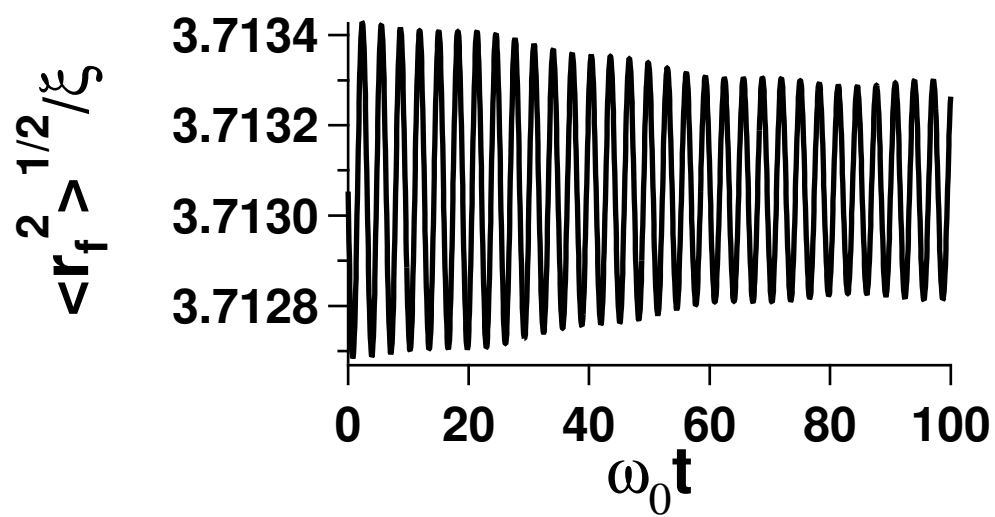


Fig.12

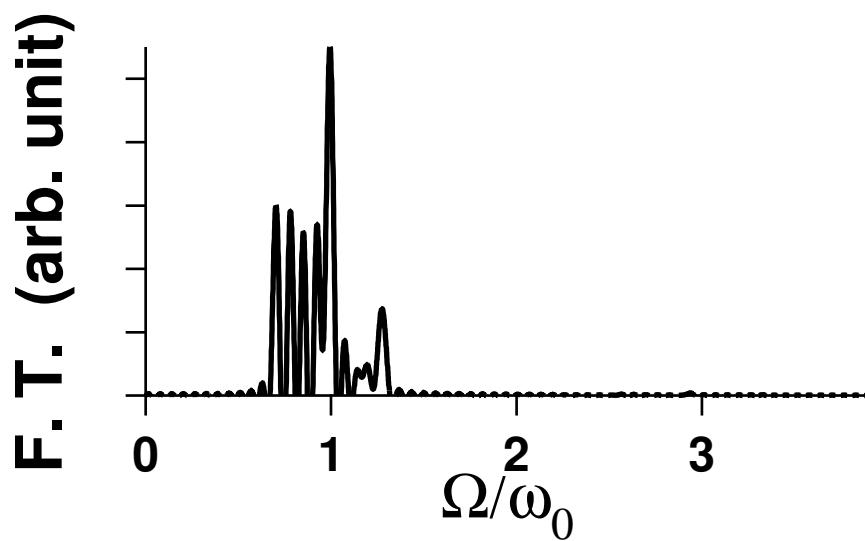
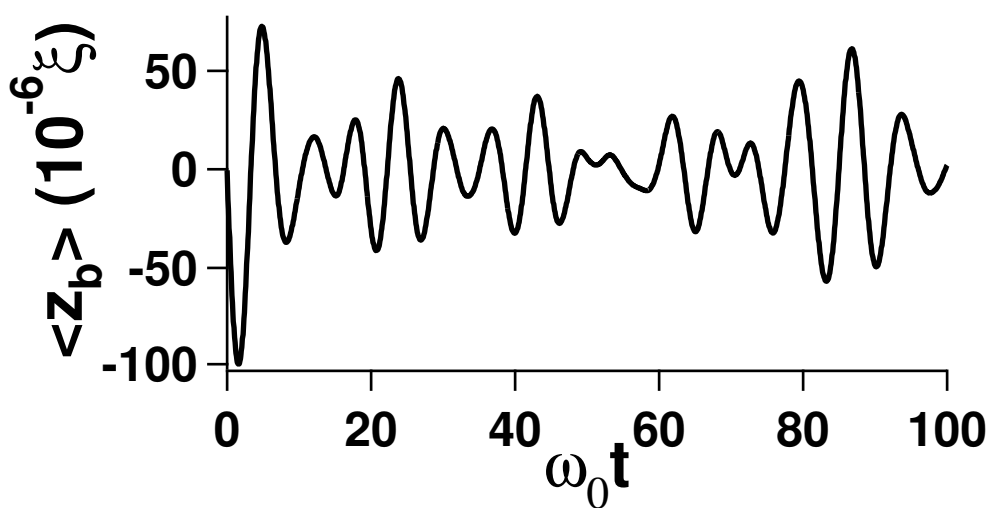
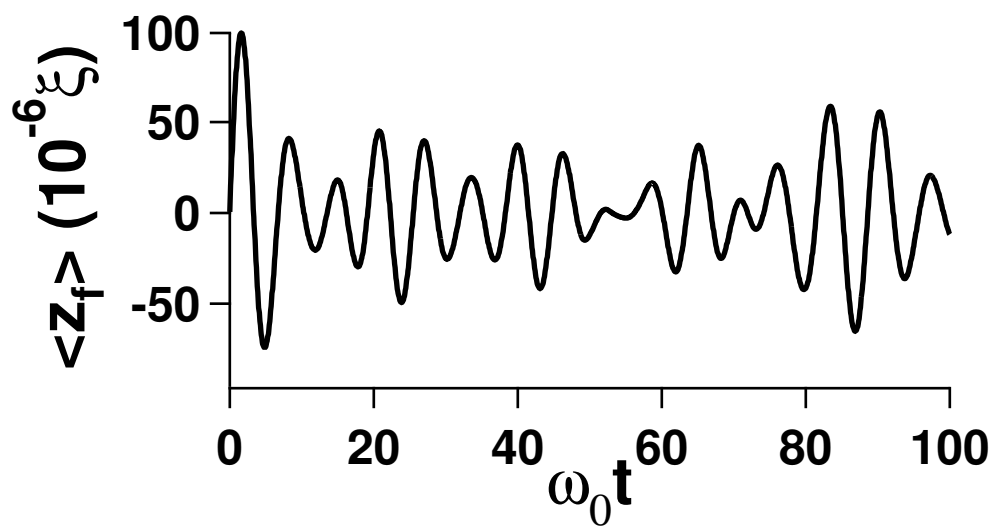


Fig.13